**IJCRT.ORG** 

ISSN: 2320-2882



# INTERNATIONAL JOURNAL OF CREATIVE RESEARCH THOUGHTS (IJCRT)

An International Open Access, Peer-reviewed, Refereed Journal

# The Continuous Strength Method For The Design Of High-Strength Built-Up Cold-Formed Beam Columns

<sup>1</sup>Salma B. Ali, <sup>2</sup>Ahmed M. Ibrahim, <sup>3</sup>Akram M. Fatouh, <sup>4</sup>Abdel Salam A. Mokhtar Department of Structural Engineering, Ain Shams University, Cairo, Egypt

Abstract: Back-to-back built-up cold-formed channel sections made of high strength steel are becoming increasingly popular for column members in cold-formed steel structures. Standard design codes put limits on slenderness ratio for designing such sections where the slenderness of single section does not exceed half of the slenderness of the back-to-back column. This paper investigates slenderness ratios beyond this limit. ABAQUS is used to conduct parametric study involving fifty-six validated models to study the exceeded limits. The effect of fastener spacing on the axial strength of back-to-back built-up columns is investigated to exceed slenderness ratio limits. The study finds that the design according to the standard codes is conservative for columns that fail through local buckling. The aim of this research is to use a new design approach, the Continuous Strength Method, to develop an equation to help exceed limits.

**Keywords:** Beam-column, Combined loading, CSM, Continuous Strength Method, Flexural buckling, Local buckling, Cold-Formed steel, Strain hardening.

#### I. INTRODUCTION

This research paper provides an in-depth analysis based on fifty-six validated finite element analyses performed on back-to-back built-up cold-formed steel (CFS) channel sections connected together with intermediate fasteners spacings subjected to compressive forces while exceeding slenderness ratio recommended by AISI [1]  $\left(\frac{s}{r_{yc}}\right) \le 0.5 \left(\frac{\kappa L}{r}\right)_o$  to overcome conservativity of current used equations. The study carefully examines the structural behavior and performance of these sections when used as columns.

Continuous strength method (CSM) has been chosen as a design approach to fulfill the aim of the research. CSM provides better results for high strength steel with rounded stress-strain curve adapted in this study.

# 1.1 General Arrangement and Cross-Sectional Details

As illustrated in Fig. 1, back-to-back channel sections are reinforced with intermediate fasteners distributed along their length. These fasteners play a crucial role in preventing independent buckling of the individual channel sections, thereby enhancing the overall stability and load-bearing capacity of the built-up columns.

The study emphasizes the significance of considering the interaction between cross-section elements and the benefits of strain hardening in the design process. By incorporating these factors, the research aims to bridge the gap between theoretical design methods and practical experimental results.

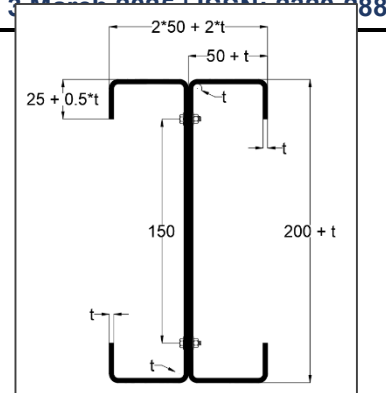


Fig. 1 Cross sectional details

# 1.2 CSM for cold-formed steel cross-section design

(CSM) is characterized by two primary features: (1) A base curve that defines the maximum level of strain  $\varepsilon_{csm}$  that a cross-section can withstand before failure due to (inelastic) local buckling, which is dependent on the slenderness of the cross-section.(2) The incorporation of a material that leverages the beneficial effects of strain hardening.

### 1.3 CSM Design Base Curve

The CSM design base curve establishes a continuous relationship between the strain ratio  $\varepsilon_{csm} / \varepsilon_y$  and the cross-section slenderness  $\lambda_p$ , where  $\varepsilon_y$  is the material yield strain equal to  $f_y/E$ , with  $f_y$  being the yield (0.2% proof) strength and E being the Young's modulus.

The definition of the cross-section slenderness  $\lambda_p$  is given by Eq. (1), where ideally the elastic buckling stress  $(\sigma_{cr})$  should be determined for the entire cross-section using numerical methods, such as finite strip software (e.g., CFS) or through approximate analytical methods.

$$\lambda p = \sqrt{\frac{f_y}{\sigma_{cr}}} \tag{1}$$

#### 1.4 Material model for cold-formed steel

To facilitate hand calculations, simple resistance functions are crucial. Yun and Gardner [2] introduced a quadlinear material model to accurately depict the characteristics of hot-rolled steels, encompassing the elastic phase, yield plateau, and strain hardening. Conversely, a bilinear (elastic and linear hardening) material model has been developed to represent the strain hardening behavior of metallic materials that exhibit a rounded stress—strain response. This includes materials such as cold-formed steels [3], austenitic and duplex stainless steels [4], ferritic stainless steels [5], and aluminum alloys [6].

The bilinear constitutive model for these metallic materials, characterized by a rounded stress–strain curve and lacking a sharply defined yield point, is illustrated in Fig. 2 as the development of the base curve [4,7,8,9].

To account for the varying strain hardening characteristics of varied materials, the slope of the linear hardening region  $E_{\rm sh}$  of the bilinear material model is determined with reference to the material coefficient  $C_{\rm i}$ . The strain hardening slope is a function of  $f_{\rm y}$ ,  $f_{\rm u}$  and  $\varepsilon_{\rm y}$ , all of which are readily available to a designer, as well as  $\varepsilon_{\rm u}$  is typically not provided in material specifications, though it can be estimated using equations. Detailed information on how these material coefficients is derived can be found in the works of Yun et al. [10] and Gardner and Yun [11] for cold-formed steels, Afshan and Gardner [4,17], Bock et al. [12] and Arrayago et al. [13] for stainless steels, and Su et al. [14,15] and Yun et al. [16] for aluminum alloys.

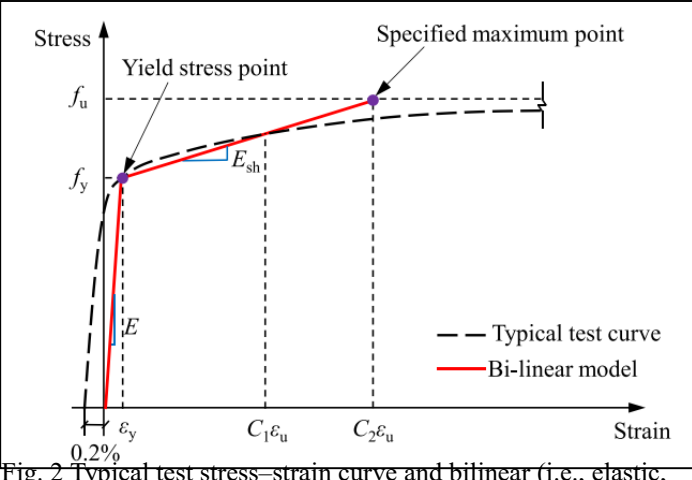


Fig. 2 Typical test stress—strain curve and bilinear (i.e., elastic, linear hardening) constitutive model for materials with a rounded stress—strain response.

# II. CSM CROSS-SECTION

#### RESISTANCE

#### **FUNCTIONS**

#### 2.1 General

Within CSM design approach, the determination of cross-section resistance relies on the limiting strain ( $\varepsilon_{csm}$ ) which is derived from the CSM base curve.  $\varepsilon_{csm}$  represents the maximum strain a cross-section can sustain before failure due to inelastic local buckling.

The suitable CSM material model incorporates the effects of strain hardening, providing a realistic representation of the material's behavior underload. By accounting for these effects, the model enhances the accuracy of strength predictions.

# 2.2 Compression

The CSM cross-section compression resistance  $N_{\rm csm,Rd}$  is determined as the product of the net cross-section area A and the CSM limiting stress  $\sigma_{\rm csm}$ , as given by:

$$N_{csm,Rd} = \frac{A\sigma_{csm}}{\gamma_{M0}} \tag{2}$$

The CSM limiting stress  $\sigma_{\rm csm}$  is calculated by substituting  $\varepsilon = \varepsilon_{\rm csm}$  into the appropriate CSM material model and determining the corresponding  $\sigma = \sigma_{\rm csm}$ , and  $\gamma_{\rm M0}$  is the partial safety factor for cross-section resistance; it has been shown that values of 1.0 and 1.1 are suitable for steel [3,18] and stainless steel [4] and aluminum alloy [14,15] design, respectively, allowing the recommended Eurocode values of  $\gamma_{\rm M0}$  to be maintained within the CSM design framework.

#### III. DESIGN RULES AS PER AISI SPECIFICATIONS AND AS/NZ STANDARDS.

The un-factored design strength of axially loaded compression members, calculated according to the AISI [1] and AS/NZ standards [21], is derived using the modified slenderness approach. This ensures that the design strength reflects the actual performance of the built-up sections under compressive loads.

$$P_{AISI} = A_e F_n \tag{3}$$

The critical buckling stress  $(F_n)$  can be calculated as follows:

$$For, \lambda c \le 1.5 : Fn = (0.658 \lambda c^2) f_v$$
 (4)

$$For, \lambda c > 1.5: Fn = \left(\frac{0.877}{\lambda c^2}\right) f_y \tag{5}$$

The non-dimensional critical slenderness ratio ( $\lambda_c$ ) can be calculated as follows:

$$\lambda c = \sqrt{\frac{f_y}{F_e}} \tag{6}$$

All the calculations above were based on the modified slenderness ratio which is calculated as per the equation below:

$$\left(\frac{KL}{r}\right)_{ms} = \sqrt{\left(\frac{KL}{r}\right)^2_o + \left(\frac{s}{r_{yc}}\right)^2} ; For which \qquad \left(\frac{s}{r_{yc}}\right) \le 0.5 \left(\frac{KL}{r}\right)_o \tag{7}$$

 $(KL/r)_{O}$  = Overall slenderness ratio of entire section about built-up member axis.

s = Intermediate fastener or spot weld spacing.

r<sub>yc</sub> = Minimum radius of gyration of full unreduced cross-sectional area of an individual shape in a builtup member

#### IV. NUMERICAL MODELING

Numerical analyses were performed using the finite element (FE) software ABAQUS [19] to simulate the behavior of cross-sections in cold-formed steel back-to-back built-up channel sections. The FE models developed for this study underwent validation against existing experimental data for cold-formed steel built-up back-to-back channel columns [20].

The validation process ensured that the developed FE models accurately represented the physical behavior of the built-up channel sections. By comparing the simulation results with experimental data, the models were refined and confirmed to be dependable for further analysis.

# 4.1 Description of the FE model

The entire geometry of the test specimens was meticulously modeled to ensure accuracy in the simulations. Contact surfaces were established between the web surfaces of the channel sections in the built-up configuration to replicate the real-world interactions.

The axial load was applied at the center of gravity of the specimens using a displacement-controlled loading approach. This method ensures precise application of the load, replicating the actual loading conditions the specimens would experience.

The static RIKS method was utilized to apply displacements at both ends of the built-up column. This advanced computational technique is well-suited for solving nonlinear problems involving instability and post-buckling behavior. The loading was applied in a total of one hundred increments, allowing for detailed observation and analysis of the structural response throughout the loading process.

### 4.2 Geometry and material properties

The comprehensive geometry of both the test specimens and the parametric study models was thoroughly modeled. This detailed modeling ensured that all relevant structural features and configurations were accurately represented.

Material non-linearity as specified at section 1.2.2 illustrated in Fig. 2 was meticulously integrated into the finite element model by specifying the appropriate stress-strain values. This integration is crucial for capturing the actual behavior of the materials under various loading conditions.

Table 1 Material properties of coupon tests

		0.2% (MPa)	Proof	Stress	$f_y$	Ultimate (MPa)	Stress	fu	Modulus (GPa)	of	elasticity	E
Ting [20]	Tina					600			205			

Table 2 Material properties for parametric study

$0.2\%$ Proof Stress $f_y$ (MPa)	Ultimate Stress fu (MPa)	Modulus	of	elasticity	E
		(GPa)			
355	515	210			

### 4.3 Element type and mesh sensitivity

The channel sections were modeled using linear 4-node quadrilateral thick shell elements, specifically the S4R5 element in the finite element analysis software. This element type was selected for its ability to accurately represent the structural behavior of the channel sections.

Each surface has been divided to a suitable number of meshes to reduce analysis duration. This number was determined to be appropriate based on the results of a convergence study, ensuring that the mesh density was sufficient to capture the necessary details without compromising computational efficiency.

Mesh sensitivity analyses were conducted to verify the adequacy of the number of elements used in the model. These analyses involved varying the mesh density and observing the effect on the results to ensure that the chosen mesh configuration provided reliable and convergent results.

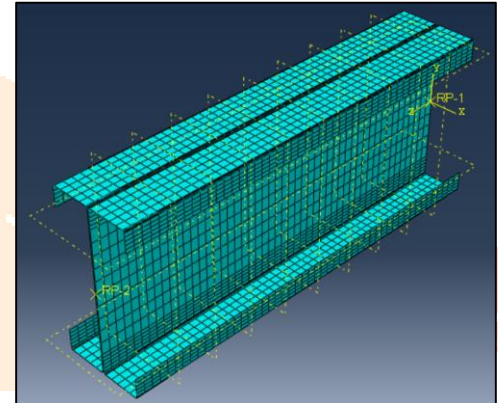


Fig. 3 Typical finite element mesh

# 4.4 Boundary conditions and load application

The back-to-back built-up cold-formed steel columns analyzed in this study were configured as pin-ended columns. To accurately define the pin-end conditions at both the upper and lower ends, displacements and rotations were restrained to the end plates through reference points.

The load was applied to the reference points of the upper end plate, as depicted in Fig. 4. This approach ensured that the load was centrally applied, replicating realistic loading conditions for the columns.

The screw connections used in the built-up columns were modeled using Cartesian basic connector elements available in the ABAQUS library. These elements accurately represented the behavior and interactions of the screw connections within the finite element model.

The load was applied incrementally using the modified RIKS method, a powerful feature in the ABAQUS library. The modified RIKS method is particularly effective for analyzing nonlinear problems, as it can predict post-buckling behavior. This capability is essential for understanding the full range of structural responses, from initial loading to potential failure modes.

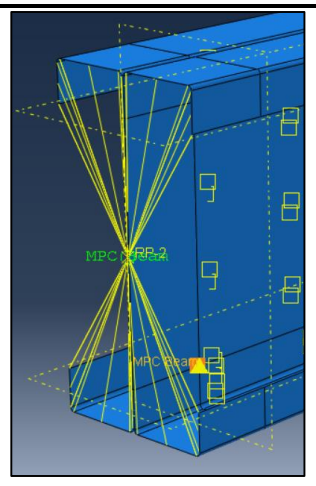


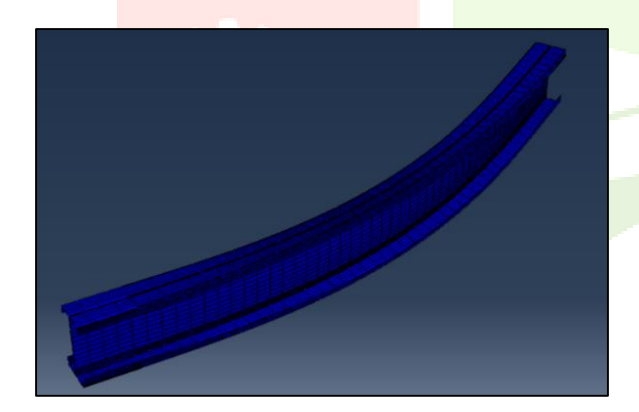
Fig. 4 Boundary condition applied to the finite element model.

# 4.5 Modelling of local and overall geometric imperfections

Eigenvalue analyses were conducted to determine the contours of global and local imperfections in the builtup cold-formed steel columns. These imperfections were scaled according to the values observed in the experimental program, ensuring that the simulations accurately reflected real-world conditions.

To replicate the experimental conditions, performed by the imperfections were scaled to match the values determined during the experimental tests. Additionally, local imperfections with a magnitude equal to 1/100 of the section height were incorporated into the finite element models. This inclusion is crucial for accurately simulating the behavior of the columns under load.

Fig. 5 in the paper illustrates the local and overall buckling modes obtained for a typical column. These visualizations serve as a validation tool, confirming the accuracy of the finite element models. They also provide valuable insights for parametric studies, helping to understand the behavior of the columns under different loading conditions and imperfections.



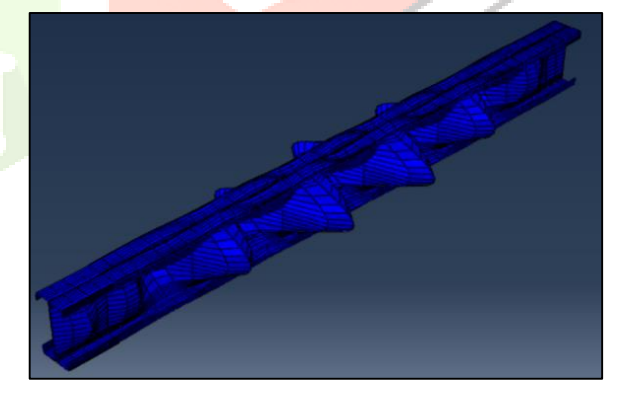


Fig. 5

a) Overall Buckling

**Initial Imperfection Contours** 

(b) Local Buckling

# 4.6 Validation of finite element model

Table 3 presents a comparison between the finite element results and the experimental data provided by validation study. The data indicates that the finite element results closely match the experimental test results. This strong correlation demonstrates that both the ultimate strength and the failure modes observed in the finite element analyses are in good agreement with the experimental findings. Consequently, the validated finite element models are deemed reliable and can be confidently used for broader parametric studies.

Table 3 Comparison with scientific paper [20]

	P <sub>test</sub> (kN)	P <sub>abaqus</sub> (kN)	P <sub>test</sub> /P <sub>abaqus</sub>
Specimen	122.5	125.935	0.973
01			
Specimen	118.5	129.678	0.914
02			
Specimen	121.9	127.203	0.958
03			

#### V. PARAMETRIC STUDY

A comprehensive parametric study was conducted, encompassing fifty-six models, utilizing a verified finite element model. The study focused on the BU200 section, which consists of back-to-back channels with dimensions of  $200 \text{ mm} \times 50 \text{ mm} \times 25 \text{ mm}$ .

The study explored several types of columns, including stub, intermediate and slender (long) columns. The thickness of these columns varied from 1.50 mm to 4.00 mm to evaluate the impact of material thickness on structural performance.

The spacing between the screws connecting the back-to-back channels varied from 50% to 100% of the overall slenderness ratio of the entire section about the built-up member axis.

Table 4 Parametric Analysis Parameters

Thickness	(1.5, 2, 3 and 4 mm)
Length	(0.5, 1, 2, 3, 4, 5 and 6 m)
Spacing (%λ)	(50,75 and 100%)

#### 5.1 Observations

The parametric study investigated the impact of slenderness ratio on various parameters, including column length, screw spacing, and column thickness.

The study observed that the slenderness ratio plays a significant role in determining the strength of the columns. As the slenderness ratio increases, the performance and stability of the columns are affected as shown in Fig. 6.

# 5.2 Comparison of design standards

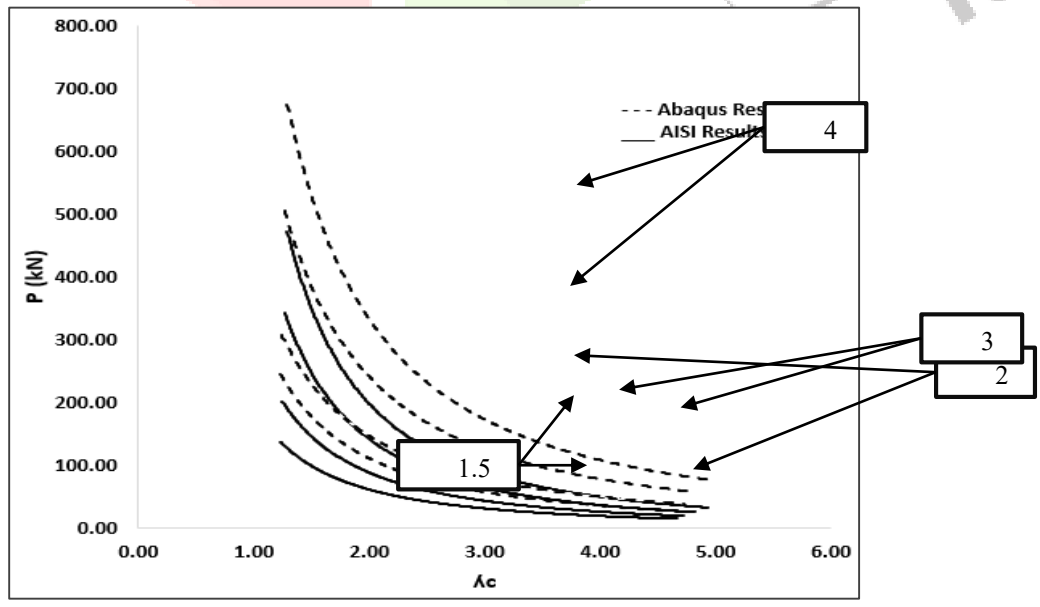


Fig. 6 Comparison of FEA and AISI& AS/NZ strengths for built up column section BU200 with different slenderness ratio.

Fig. 6 illustrates the relation between slenderness ratio  $\lambda$  and predicted compressive strength P for specimens specially presents the difference between results obtained using AISI [1] standards and results obtained by Abaqus

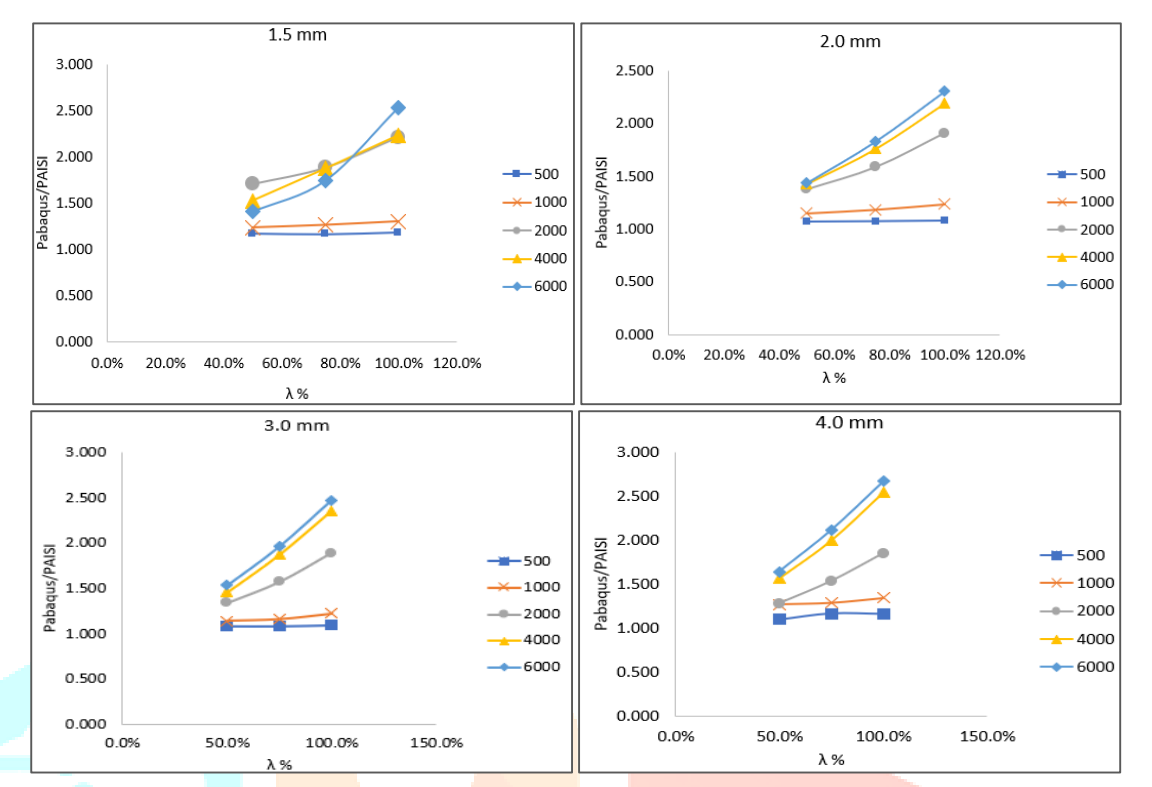


Fig. 7 Comparison with design standards results

Fig. 7 illustrates the relation between percentage of the ratio between single section slenderness and back-to-back section slenderness λ% and ratio between compressive capacity obtained by Abaqus [19] and AISI [1].

In the preliminary observations for Fig. 6 - 7, it has been noted that shorter lengths, such as 0.5 and 1.0 meters, do not exhibit significant differences in behavior compared to longer lengths. This is because shorter sections are less prone to fail due to local buckling when the slenderness ratio ( $\lambda$ ) of the section is less than 0.68.

However, for longer sections with a slenderness ratio greater than 0.68, there is a noticeable difference in behavior. These longer sections are more susceptible to local buckling, and the disparity in performance becomes more pronounced. This difference increases proportionally with the overall slenderness ratio.

For sections with a slenderness ratio exceeding 50%, the behavior becomes especially pronounced. These sections exhibit significant differences that fall outside the limits defined by standard design codes  $\left(\frac{s}{r_{yc}}\right) \le$ 

 $0.5 \left(\frac{\kappa L}{r}\right)_o$  This highlights the importance of accurately accounting for slenderness effects in the design of longer built-up sections, as they are more vulnerable to instability and buckling issues, so for that the proposed equation aims to cover that difference.

# VI. PROPOSED DESIGN RULES

Based on the results obtained from the finite element analysis (FEA), it became feasible to plot the base curve representing the relationship between the strain ratio and the slenderness ratio.

To address these discrepancies, a proposed rule was defined, introducing an equation that can be used to determine the standards' concluding section compression capacity. This equation aims to equate the difference observed between the FEA predictions and the design standards, thus providing a more accurate assessment of the compression capacity of the sections.

Strain ratio used in the plot is  $\varepsilon_{csm}$  over  $\varepsilon_y$ , where  $\varepsilon_y = E / f_y$  and  $\varepsilon_{csm} = E / f$  where f is compression force determined by FEA over the effective area computed by design standards using EWM.

Using the plot helped to develop the equation Eq. (8) that covers the required difference.

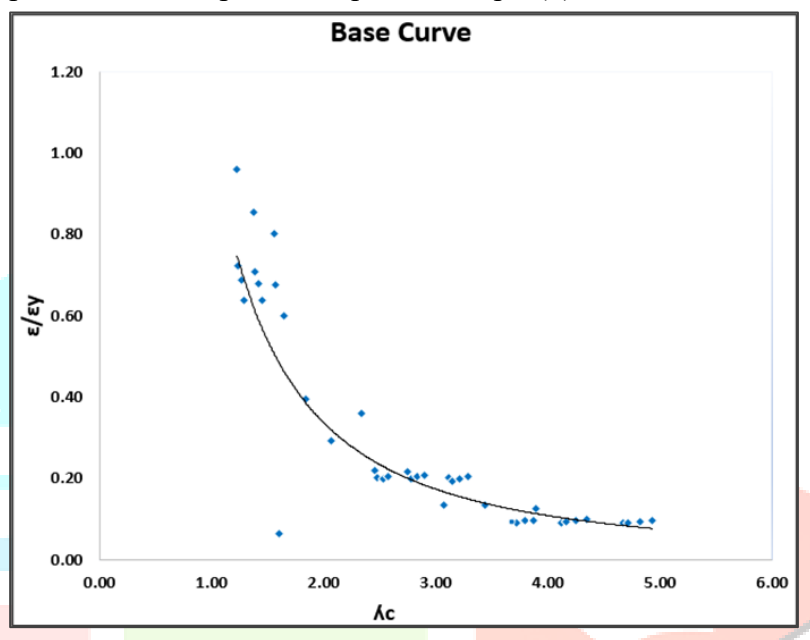


Fig. 8 Base curve for slender sections – proposed equation

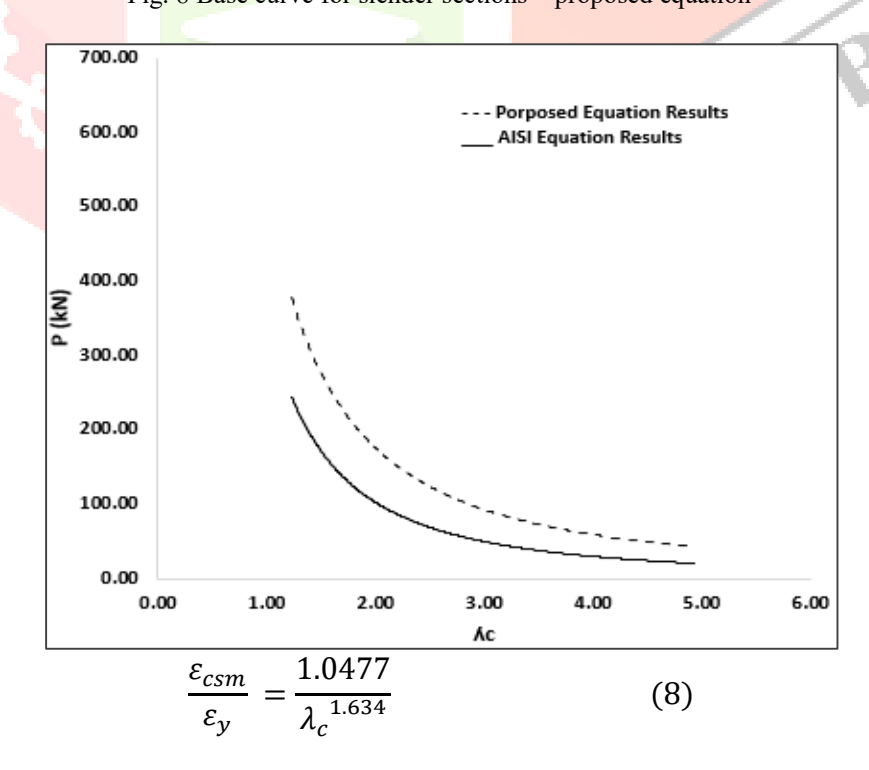


Fig. 9 Comparison between proposed equation and AISI equation

#### VII. CONCLUSION

- This paper presents the findings from fifty-six non-linear finite element analyses conducted on back-to-back built-up cold-formed steel (CFS) channels subjected to axial compression. The non-linear finite element model incorporates explicit modeling of web fasteners, material non-linearity, and geometric imperfections.
- > The results obtained from the finite element analyses were compared against existing literature, and a good agreement was observed. This validation underscores the reliability and accuracy of the finite element models used in this study.
- ➤ Following the validation, finite element models were employed to perform parametric study. This study investigated the impact of several factors, including. The effect of different material thicknesses on the behavior of the built-up columns.
- The influence of varying screw spacings on structural performance The role of slenderness in the stability and strength of the columns.
- > The column strengths obtained by the finite element analyses were compared with the design strengths calculated in accordance with the AISI and AS/NZS standards. The comparison revealed that the design standards tend to be conservative for all columns, often underestimating their actual strength.
- > The effect of changing the screw spacing only affects the mode of buckling failure and so the slenderness ratio modified by standard codes.
- The effect of using CSM determining the compression capacity of sections leads to a more optimized design and helps decrease the costs of using such sections.
- Local or Global buckling failure mode depends on the screw spacing, the channel geometry and specimen length.
- The proposed equation can predict different configurations of cold-formed steel built-up back-to-back channel beam columns for compression capacity.

#### VIII. REFERENCES

- [1]. American Iron and Steel Institute (AISI). North American Specification for the Design of Cold-formed Steel Structural Members. AISI; 2007. p. S100–7.
- [2]. Yun X, Gardner L. Stress-strain curves for hot-rolled steels. J Constr Steel Res 2017;133:36–46.
- [3]. Yun X, Gardner L. The continuous strength method for the design of cold-formed steel non-slender tubular cross-sections. Eng Struct 2018;175:549–64.
- [4]. Afshan S, Gardner L. The continuous strength method for structural stainless steel design. Thin-Walled Struct 2013;68:42–9.
- [5]. Bock M, Gardner L, Real E. Material and local buckling response of ferritic stainless steel sections. Thin-Walled Struct 2015;89:131–41.
- [6]. Su MN, Young B, Gardner L. The continuous strength method for the design of aluminium alloy structural elements. Eng Struct 2016;122:338–48.
- [7]. Gardner L. The continuous strength method. Proc Inst Civ Eng: Struct Build 2008; 161(3):127–33.
- [8]. Gardner L, Ashraf M. Structural design for non-linear metallic materials. Eng Struct 2006;28(6):926–34.
- [9]. Ashraf M, Gardner L, Nethercot DA. Structural stainless steel design: resistance based on deformation capacity. J Struct Eng ASCE 2008;134(3):402–11.
- [10]. Yun X, Gardner L. The continuous strength method for the design of cold-formed steel non-slender tubular cross-sections. Eng Struct 2018;175:549–64.
- [11]. Gardner L, Yun X. Description of stress-strain curves for cold-formed steels. Constr Build Mater 2018;189:527–38.
- [12]. Bock M, Gardner L, Real E. Material and local buckling response of ferritic stainless steel sections. Thin-Walled Struct 2015;89:131–41.
- [13]. Arrayago I, Real E, Gardner L. Description of stress-strain curves for stainless steel alloys. Mater Des 2015;87:540–52.
- [14]. Su MN, Young B, Gardner L. The continuous strength method for the design of aluminium alloy structural elements. Eng Struct 2016;122:338–48.
- [15]. Su MN, Young B, Gardner L. Testing and design of aluminum alloy cross-sections in compression. J Struct Eng ASCE 2014;140(9):04014047.
- [16]. Yun X, Wang ZX, Gardner L. Full-range stress-strain curves for aluminum alloys. J Struct Eng ASCE 2021;147(6):04021060.

- [17]. Afshan S, Zhao O, Gardner L. Standardised material properties for numerical parametric studies of stainless steel structures and buckling curves for tubular columns. J Constr Steel Res 2019;152:2–11.
- [18]. Yun X, Gardner L, Boissonnade N. The continuous strength method for the design of hot-rolled steel cross-sections. Eng Struct 2018;157:179–91.
- [19]. ABAQUS. Analysis User's Manual-Version 6.14-2. USA: ABAQUS Inc.; 2014.
- [20]. Ting, Tina & Lau, Hieng Ho. (2011). Compression Test on Cold-Formed Steel Built-Up Back-to-Back Channels Stub Columns. Advanced Materials Research. 201-203. 2900-2903.
- [21]. Australia/New Zealand Standard (AS/NZS). Cold-formed Steel Structures, AS/NZS 4600:2005. Standards Australia/Standards New Zealand; 2005.

